Journal of Sound and Vibration 329 (2010) 673–686

Contents lists available at ScienceDirect

Journal of Sound and Vibration

journal homepage: www.elsevier.com/locate/jsvi

Sound transmission loss of foam-filled honeycomb sandwich panels using statistical energy analysis and theoretical and measured dynamic properties

Ran Zhou *, Malcolm J. Crocker

Department of Mechanical Engineering, Auburn University, Auburn, AL 36849, USA

ARTICLE INFO

Article history:
Received 15 June 2009
Received in revised form
14 September 2009
Accepted 2 October 2009
Handling Editor: A.V. Metrikine
Available online 28 October 2009

ABSTRACT

Comparisons between the experimental and predicted sound transmission loss values obtained from statistical energy analysis are presented for two foam-filled honeycomb sandwich panels. Statistical energy analysis (SEA) is a modeling procedure which uses energy flow relationships for the theoretical estimation of the sound transmission through structures in resonant motion. The accuracy of the prediction of the sound transmission loss using SEA greatly depends on accurate estimates of: (1) the modal density, (2) the internal loss factor, and (3) the coupling loss factor parameters of the structures. A theoretical expression for the modal density of sandwich panels is developed from a sixth-order governing equation. Measured modal density estimates of the two foam-filled honeycomb sandwich panels are obtained by using a three-channel spectral method with a spectral mass correction to allow for the mass loading of the impedance head. The effect of mass loading of the accelerometer is corrected in the estimations of both the total loss factor and radiation loss factor of the sandwich panels.

1. Introduction

Vibration and transmission of sound through structures are of concern with many mechanical systems including aerospace and surface transportation vehicles, building structures, industrial machinery and home appliances [1–5]. Many such structures are comprised of beam and panel like elements. The vibration of beam and panel systems can be reduced by the use of passive damping, once the system parameters, such as the dynamic stiffness of the panels or beams, have been identified [6–8]. Alternatively, attempts can also be made to suppress vibration, sound radiation and transmission of sound through such structures through a thorough understanding of the vibration using approaches such as statistical energy analysis [9]. It is necessary to identify the panel or beam system parameters no matter what methods of noise and vibration control are chosen.

Composite sandwich structures have been increasingly used in recent years instead of metal structures for the construction of aircraft, spacecraft and ships, because of their high stiffness-to-weight ratios, lack of corrosion and the introduction of a viscoelastic core layer, which has high inherent internal damping. This trend is dictated by demands for high load capacity and reduced fuel consumption for cars and trucks and aerospace structures [2,6–8]. It is important to understand and to be able to predict the transmission of sound through such structures in order to protect the occupants in aircraft and vehicle cabins from the noise of the powerplants. Although composite sandwich panels normally have higher

* Corresponding author. Tel.: +1 334 844 3455.
E-mail address: zhouran@auburn.edu (R. Zhou).

0022-460X/$ - see front matter © 2009 Elsevier Ltd. All rights reserved.
doi:10.1016/j.jsv.2009.10.002

internal damping than metal structures. This is useful in reducing resonant vibration. Unfortunately, however, they often have poorer sound transmission properties than metal panels, since the coincidence region can extend over a much greater frequency range than metal panels.

Statistical energy analysis (SEA) is a modeling procedure which uses energy flow relationships for the theoretical estimation of the vibration response levels of structures in resonant motion and for the noise radiation from and the sound transmission through these structures. The accuracy of the prediction of the response and the sound transmission loss of structures using SEA greatly depends on an accurate estimates of (1) the modal density, (2) the internal loss factor, and (3) the coupling loss factor parameters of the structures. A large number of researchers have studied these three parameters of single-layer structures. Only a limited amount of work, however, has been carried out to determine these parameters for sandwich panels.

In principle, the modal density can be obtained experimentally by exciting the structure with a sinusoidal force of varying frequency and counting the number of modes that are excited in each frequency band. However, the mode count method is not suitable for structures that have a high modal density and a high modal overlap or those in which heavily damped modes are present. Because of these reasons, the point mobility method, described by Cremer et al. [10] is a more suitable for measuring modal densities. The accuracy of this method is critically dependent on the reliable measurement of force and velocity. Clarkson and Pope [11] employed this method to estimate the modal density of plates and cylinders, and found that the real part of the point mobility of very lightly damped structures can be negative.

Brown [12] showed that modal density experimental estimates can be improved by using a three-channel spectral method which minimizes the erroneous results generated by feedback noise caused by exciter-structure interaction. The mass loading which results from the added mass that appears between the impedance head and the structure can affect the point mobility transfer function. Brown and Norton [13] showed that the modal density measurement for cylindrical pipes can be further improved by using a three-channel spectral method with a mass correction applied to the point mobility measurement. Keswick and Norton [14] used two mass correction methods, the measured mass method and the spectral mass method, to obtain the experimental modal densities of a lightly damped clamped cylindrical pipe. Their results showed that the spectral mass method is in better agreement with theory than the measured mass method.

Clarkson and Ranky [15] derived an expression for the modal density of honeycomb sandwich panels from a reduced form of the governing equation for sandwich structures presented by Mead and Markus [16] and they evaluated the modal density of honeycomb panels experimentally by using a two-channel spectral method without using a mass correction. Renji and Nair [17] developed an expression for the modal density of a symmetric sandwich panel from a fourth-order equation which was modified from the governing equation for a symmetric laminate by including the shear flexibility of the core. In their work, they considered both real and imaginary parts of the point mobility in the measured mass correction.

The expressions for the modal density of honeycomb sandwich panels given by both Clarkson and Ranky [15] and Renji and Nair [17] were developed from fourth-order governing equations, while most governing equations for symmetric honeycomb sandwich panels are sixth-order [16,28–30]. Ferguson and Clarkson [18] presented an expression for the modal density of honeycomb sandwich panels derived from the sixth-order equation presented by Mead and Markus [16]. However, there is an error in their expression.

There are two direct experimental techniques for obtaining internal loss factors that are often used. These are: (1) the half-power bandwidth method and (2) the envelope decay method. Only the internal loss factors of the non-overlapping modes can be obtained from the half-power bandwidth method. For SEA applications, the primary property of interest is the band-averaged loss factor, not the modal loss factor. The envelope decay method is based on determining the logarithmic decrement of the transient structural response. This is obtained from measurements of the decay of the vibration after the excitation is cut off. The steady-state power flow method is an indirect experimental approach to obtain the band-averaged loss factor.

Clarkson and Pope [11] showed that the band-averaged loss factor of a cylinder, calculated from the power flow method, is higher than that obtained from the envelope decay method. Ranky and Clarkson [19] found that there is no significant difference between the results from the two methods when the modes in the chosen band of frequency have similar modal loss factors. If this is not the case, the decay curve is not a straight line; then the power flow method provides the result required for SEA calculations. Renji and Narayan [20] investigated loss factors of honeycomb sandwich panels. They corrected their results for the effect of added mass on the driving force by using the measured mass correction method and assumed that the mass loading of the accelerometer, which was employed to measure the spatial velocity of the panel, is negligible.

Most experiments used to measure the loss factor of a structure have been conducted in air. In such cases, the loss factor reported is the total loss factor, which includes the radiation loss factor. Lyon and Maidanik [21,22] developed an expression for the radiation resistance of a baffled simply supported panel excited in a reverberant acoustic field. They also described how the radiation loss factor of a structure in a reverberant field can be determined experimentally [22]. Crocker and Price [23] presented an experimental method to determine the radiation loss factor of a structure clamped between two reverberation rooms. Gomperts [24] provided an expression for the radiation efficiency of a baffled free-edge panel and Oppenheimer and Dubowsky [25] studied the radiation efficiency of an unbaffled simply supported panel. Both of these studies were based on the results developed by Maidanik [22]. Very little published data exist on the radiation loss factors or radiation resistances of composite sandwich panels.

Crocker and Price [23] presented general power flow relationship equations for a room–panel–room transmission suite. The power flow between the two rooms was defined as the flow between non-resonant modes, when there are no modes excited in the panel in the frequency band under consideration. Both non-resonant and resonant vibration modes were taken into consideration. Sewell [26] derived an expression for the forced vibration transmission coefficient of a baffled single-layer partition in a reverberant acoustic field using a classical approach. Sewell's expression is generally valid when the surface density of the partition is greater than $10\,\mathrm{kg\,m^{-2}}$.

In this study, the modal densities of a honeycomb sandwich panel and two foam-filled honeycomb sandwich panels are computed. The experimental values of the modal density, total loss factor, and radiation resistance of the two foam-filled honeycomb sandwich panels are presented. Finally comparisons between the experimental and predicted sound transmission loss values obtained from statistical energy analysis are presented for the two foam-filled honeycomb sandwich panels.

2. Theoretical expression for modal density

The modal density of structures depends on their boundary conditions and the governing equations of motion. For simply supported panels, the modal density is associated with the constant frequency loci of the wavenumber; then

$$n(f) = 2\pi \frac{(\pi/4)\Delta k^2}{(\pi/l_x)(\pi/l_y)\Delta\omega} = \frac{A_p}{2}\frac{\mathrm{d}k^2}{\mathrm{d}\omega}, \tag{1}$$

where l_x and l_y are the dimensions of the panel and A_p the surface area of the panel.

The modal density of sandwich panels is more complicated because not only is it frequency dependent, but this frequency dependence is not a linear function. Most governing equations for sandwich structures have been developed by assuming that the panel elements or beam elements are one-dimensional [16,27–30]. Both anti-symmetric and symmetric motion of the face sheets has been considered to describe the motion of sandwich panels [27–29]; only anti-symmetric motion is normally included in the development of the governing equation for sandwich beams [16,30].

For sandwich panels with stiff cores, such as honeycomb cores, the anti-symmetric motion is dominant in the frequency band under consideration. The governing equation for anti-symmetric motion of sandwich panels can be written as a cubic equation with respect to k^2,

$$k^6 + a_2 k^4 + a_1 k^2 + a_0 = 0. \tag{2}$$

In the absence of damping, the wavenumber of free anti-symmetric transverse motion is always real. Then the propagating wavenumber must satisfy the equation,

$$k^2 = -\frac{a_2}{3} + (S+T), \tag{3}$$

where

$$S = \sqrt[3]{R+\sqrt{D}}, \quad T = \sqrt[3]{R-\sqrt{D}}, \quad D = Q^3 + R^2,$$

$$Q = \frac{3a_1 - a_2^2}{9}, \quad R = \frac{9a_2a_1 - 27a_0 - 2a_2^3}{54}.$$

Hence the modal density can be obtained from

$$\frac{\mathrm{d}k^2}{\mathrm{d}\omega} = \left[-\frac{1}{3}\frac{\mathrm{d}a_2}{\mathrm{d}\omega} + \left(\frac{\mathrm{d}S}{\mathrm{d}\omega} + \frac{\mathrm{d}T}{\mathrm{d}\omega}\right)\right], \tag{4}$$

$$\text{with } \frac{\mathrm{d}S}{\mathrm{d}\omega} = \frac{1}{3}S^{-2}\left(\frac{\mathrm{d}R}{\mathrm{d}\omega} + \frac{1}{2\sqrt{D}}\frac{\mathrm{d}D}{\mathrm{d}\omega}\right), \quad \frac{\mathrm{d}T}{\mathrm{d}\omega} = \frac{1}{3}T^{-2}\left(\frac{\mathrm{d}R}{\mathrm{d}\omega} - \frac{1}{2\sqrt{D}}\frac{\mathrm{d}D}{\mathrm{d}\omega}\right),$$

$$\frac{\mathrm{d}D}{\mathrm{d}\omega} = 3Q^2\frac{\mathrm{d}Q}{\mathrm{d}\omega} + 2R\frac{\mathrm{d}R}{\mathrm{d}\omega}, \quad \frac{\mathrm{d}R}{\mathrm{d}\omega} = \frac{a_1}{6}\frac{\mathrm{d}a_2}{\mathrm{d}\omega} + \frac{a_2}{6}\frac{\mathrm{d}a_1}{\mathrm{d}\omega} - \frac{1}{2}\frac{\mathrm{d}a_0}{\mathrm{d}\omega} - \frac{a_2^2}{9}\frac{\mathrm{d}a_2}{\mathrm{d}\omega},$$

$$\frac{\mathrm{d}Q}{\mathrm{d}\omega} = \frac{1}{3}\frac{\mathrm{d}a_1}{\mathrm{d}\omega} - \frac{2a_2}{9}\frac{\mathrm{d}a_2}{\mathrm{d}\omega}.$$

Eq. (2) is equivalent to the sixth-order governing equation for free motion of sandwich structures presented by Mead and Markus [16], if

$$a_2 = g(1+Y), \quad a_1 = -\frac{\mu}{D_t}\omega^2, \quad a_0 = -\frac{\mu}{D_t}g\omega^2, \tag{5}$$

$$\text{with } Y = \frac{[h+(t_1+t_3)/2]^2E_1t_1E_3t_3}{D_t(E_1t_1+E_3t_3)}, \quad g = \frac{G_c}{h}\left(\frac{1}{E_1t_1} + \frac{1}{E_3t_3}\right), \quad D_t = \frac{E_1t_1^3 + E_3t_3^3}{12},$$

where E_j is the Young's modulus of the face sheet j; G_c the out-of-plane shear modulus of the core; t_j and h are the thickness of the face sheet j and the core, respectively; and μ the mass per unit area of the sandwich panel.

Clarkson and Ranky [15] treated honeycomb sandwich panels as equivalent flat plates to derive the modal density, $n(f)$, by assuming that the bending rigidity of the face sheets, D_t, is negligible in the sixth-order equation given by Mead and Markus,

$$n(f) = \frac{\pi\mu A_p f}{gD_t(1+Y)}\left(1 + \frac{\mu\omega^2 + 2g^2D_t(1+Y)}{\sqrt{(\mu\omega^2)^2 + 4\mu(g\omega)^2D_t(1+Y)}}\right). \tag{6}$$

For a honeycomb core, with different out-of-plane shear moduli, Clarkson and Ranky used $\sqrt{G_xG_y}$ to make an estimation of the shear modulus of the honeycomb core, G_c, where G_x and G_y are the out-of-plane shear moduli of the core.

Ferguson and Clarkson [18] presented an analytical expression for the modal density of a sandwich panel derived from the governing equation given by Mead and Markus by expressing Eq. (3) in terms of radicals,

$$n(f) = \frac{A_p}{9}\left\{P^{-2/3}\frac{\mathrm{d}P}{\mathrm{d}\omega}\cos\frac{\theta}{3} - P^{1/3}\sin\frac{\theta}{3}\frac{\mathrm{d}\theta}{\mathrm{d}\omega}\right\}. \tag{7}$$

There is an error in their expression for the parameter P. The correct expression for P should be as follows:

$$P = 3\sqrt{3}\left\{\frac{\mu\omega^2}{D_t} + \frac{1}{3}g^2(1+Y)^2\right\}^{3/2}. \tag{8}$$

The factor of the second term in the curly brackets of the expression for P given by Ferguson and Clarkson is $\frac{1}{2}$, not $\frac{1}{3}$.

Renji and Nair [17] developed a governing equation for a symmetric orthotropic laminate with an isotropic core from the governing equation of motion for a symmetric laminate by including the shear flexibility of the core.

$$D_{11}\frac{\partial^4 w}{\partial x^4} + 2(D_{12} + 2D_{66})\frac{\partial^4 w}{\partial x^2\partial y^2} + D_{22}\frac{\partial^4 w}{\partial y^4} = -\frac{1}{N}\left(D_{11}\frac{\partial^4 q}{\partial x^4} + D_{22}\frac{\partial^4 q}{\partial y^4}\right) + q, \tag{9}$$

where D_{ij} is the flexural rigidity of the sandwich structure; N the shear rigidity of the core; and q the force per unit area of the structure.

The governing equation for the forced vibration of sandwich structures given by Mead and Markus [29], is

$$\frac{\partial^6 w}{\partial x^6} - g(1+Y)\frac{\partial^4 w}{\partial x^4} = \frac{1}{D_t}\left(\frac{\partial^2 q}{\partial x^2} - gq\right). \tag{10}$$

It is noted that by neglecting the highest partial differential term, the above equation reduces to

$$D_t(1+Y)\frac{\partial^4 w}{\partial x^4} = -\frac{1}{g}\frac{\partial^2 q}{\partial x^2} + q. \tag{11}$$

Thus, Eq. (9) is a two-dimensional version of Eq. (11). For sandwich panels with isotropic materials, these two equations are equivalent. The expression for the modal density of sandwich panels with orthotropic face sheets given by Renji and Nair requires knowledge of the off-axis stiffness values of the face sheets to obtain the off-axis flexural rigidity values, D_{12} and D_{66}.

The modal densities of sandwich panel A, with plywood face sheets and paper honeycomb core are presented in Fig. 1. The properties of sandwich panel A given by Moore and Lyon [29] are presented in Table 1. The equivalent out-of-plane shear modulus G_c was chosen as the value of G_x to illustrate the effect of the bending rigidity of the face sheets D_t on the modal density of sandwich panel A.

The critical frequency of a structure is the lowest frequency at which the phase speed of structural transverse waves is equal to the speed of sound in the fluid. The fluid is air in most applications. The critical frequency of transverse waves in the x-axis direction of panel A obtained from the governing equation given by Mead and Markus, occurs near to 250 Hz. It is seen that the effect of the contribution of the bending rigidity of the face sheets D_t on the modal density of sandwich panel A is important above 2000 Hz, above the critical frequency. Eq. (6) overestimates the modal density and the approximate value can be twice that of the modal density computed from Eqs. (4) and (5), or Eqs. (7) and (8) above 4000 Hz.

3. Experimental modal densities

The modal density of a structure can be obtained from the measurement of the spatially averaged point mobility frequency response function. The band-averaged modal density is given by [10],

$$n(f) = \frac{1}{\Delta f}\int 4M_p\overline{\mathrm{Re}[Y(f)]}\,\mathrm{d}f, \tag{12}$$

where $Y(f) = V(f)/F(f)$ is the point mobility of the structure; M_p the mass of the structure, and Δf the frequency analysis bandwidth.

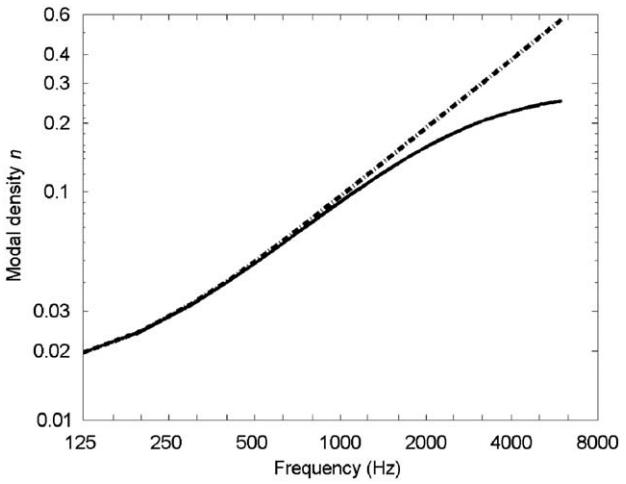

Fig. 1. Modal densities of propagating transverse wave in sandwich panel *A*, $G_c = G_x$: —— Eqs. (4) and (5) or Eqs. (7) and (8); – · – · – Eq. (6).

Table 1
Properties of sandwich panels *A*, *B* and *C*.

Property	Panel *A* [29]	Panel *B*	Panel *C*
Face sheet			
Density (kgm^{-3})	657	1600	1600
Young's modulus E_t (GPa)	7.7	49	39
Poisson's ratio	0.3	0.15	0.15
Thickness t (mm)	6.35	0.5	0.5
Core			
Density (kgm^{-3})	28	160	120
Thickness h (mm)	76.2	6.35	12.7
Out-of-plane shear modulus G_x (MPa)	24	90	100
Out-of-plane shear modulus G_y (MPa)	52	140	60
Poisson's ratio	0.15	0.15	0.15
Dimensions $l_x \times l_y$ (m × m)	1.22 × 2.44	1.12 × 0.62	1.12 × 0.62

In the three-channel spectral method, the point mobility is determined by using the relation,

$$Y(f) = \frac{G_{sv}(f)}{G_{sf}(f)}, \tag{13}$$

where $G_{sv}(f)$ and $G_{sf}(f)$ are the cross-spectra between the original input and the measured velocity, and the original input and the measured force.

Mass corrections must be considered when making any frequency response measurements on a lightweight structure. In the case of point mobility measurements, there will always be some added mass present between the force gauge of the impedance head and the structure. The added mass will corrupt the force measurement because some portion of the force measured is used to drive against the inertial resistance of the added mass.

The point mobility measurement can be corrected for the mass loading effect as follows:

$$Y_c = \frac{V_m}{F_c} = \frac{V_m}{F_m - MA_m} = \frac{V_m/F_m}{1 - \mathrm{i}\omega M V_m/F_m} = \frac{Y_m}{1 - \mathrm{i}\omega M Y_m}, \tag{14}$$

where A_m and F_m are the acceleration and force measured by the impedance head; V_m and Y_m are the measured velocity and point mobility; F_c and Y_c are the corrected force and point mobility; and M is the added mass between the force gauge and the structure.

The added mass M can be evaluated by adding the manufacturer's specifications for the mass below the force gauge to the mass of the attachment components or by measuring the point mobility of the added mass attached to the impedance head when it is separated from the structure. The first correction method is termed as the measured mass method. The second correction method is termed as the spectral mass method.

Hence, the real and imaginary components of the corrected point mobility are

$$\mathrm{Re}(Y_c) = \frac{\mathrm{Re}(Y_m)}{[1+\omega M \mathrm{Im}(Y_m)]^2 + [\omega M \mathrm{Re}(Y_m)]^2}, \tag{15}$$

$$\mathrm{Im}(Y_c) = \frac{\omega M\{[\mathrm{Im}(Y_m)]^2 + [\mathrm{Re}(Y_m)]^2\} + \mathrm{Im}(Y_m)}{[1+\omega M \mathrm{Im}(Y_m)]^2 + [\omega M \mathrm{Re}(Y_m)]^2}. \tag{16}$$

In this study, the modal density of the sandwich panels studied was obtained by averaging the modal densities measured at four randomly chosen points on the panels. The point mobility was measured at each position with a B&K impedance head type 8000 that was attached to a B&K vibration exciter type 4809 by a stud. The impedance head was attached to the panel with wax. The sandwich panel was suspended by strings and excited by the exciter with a broadband random force, as shown in Fig. 2.

The measured inertance of the added mass between the force gauge and the panel was found to be between 860 and 960 $\mathrm{ms^{-2}\,N^{-1}}$ in the frequency band, 200−5600 Hz. Then the effective dynamic mass of the added mass was calculated to be between 1.06 and 1.14 g, which is slightly smaller than 1.2 g, the mass below the force gauge of the impedance head specified by the manufacturer. The frequency spectral analysis resolution was chosen to be 1 Hz. Two frequency analysis bandwidths Δf, were chosen (1) one-third octave and (2) a constant bandwidth of 400 Hz. The first is consistent with most previous work and the second was chosen to ensure that there are at least five resonance frequencies in each analysis band.

Two sandwich panels with plane weave fabric-reinforced graphite composite face sheets and polyurethane (PUR) foam-filled honeycomb core, panels *B* and *C*, were investigated. Plain weave is the most stable construction used for composite face sheets and has minimum slippage. The strength is approximately the same in the two principal directions. The combination of PUR foam and honeycomb materials gives the core the advantage of possessing both foam and honeycomb properties, a high shear modulus, and a large bonding area. The properties of panels *B* and *C*, are given in Table 1.

For boundary conditions, other than simply supported, analytical expressions for the eigenmodes of panels in free vibration are not available. Higher order eigenmodes of the free vibration of panels are less sensitive to boundary conditions than lower order eigenmodes. Thus, except for the first several eigenmodes, the modal density for simply supported panels provides a good approximation for that of panels with other boundary conditions.

Figs. 3 and 4 show the experimental estimates of the modal density for panels *B* and *C*. It is seen that the mass loading effect of the mass below the force gauge on the measurement of point mobility is apparent above 2000 Hz for the two foam-filled honeycomb sandwich panels. Two lines are indicated in Figs. 3 and 4. The solid lines correspond to theoretical modal density predictions of the two panels made using $G_c = G_x$. The dashed lines represent theoretical modal density predictions of the two panels made using $G_c = G_y$. The critical frequencies of panels *B* and *C* obtained from the governing equation given by Mead and

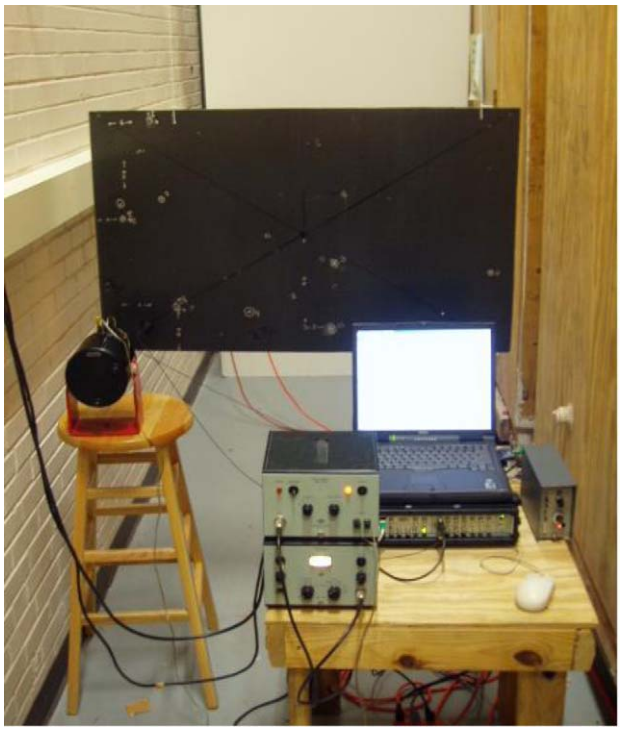

Fig. 2. Set-up for the modal density, total loss factor and radiation resistance experiments of panels with free edges.

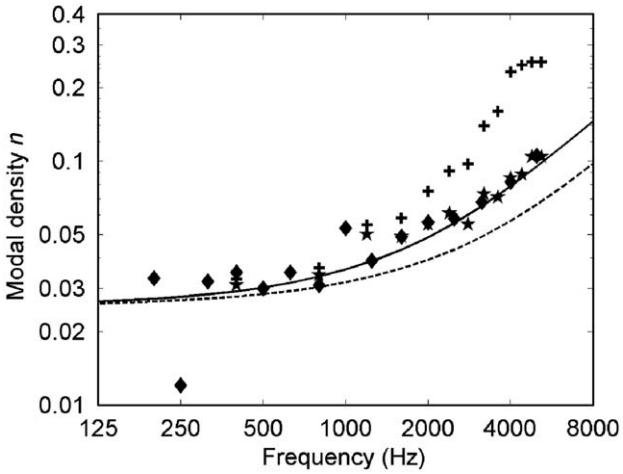

Fig. 3. Band-averaged modal density estimates for sandwich panel *B*: ♦ one-third octave bandwidth; ★ 400 Hz bandwidth; + 400 Hz bandwidth without mass correction; —— theoretical estimates by using Eq. (6) and $G_c = G_x$; – – – theoretical estimates by using Eq. (6) and $G_c = G_y$.

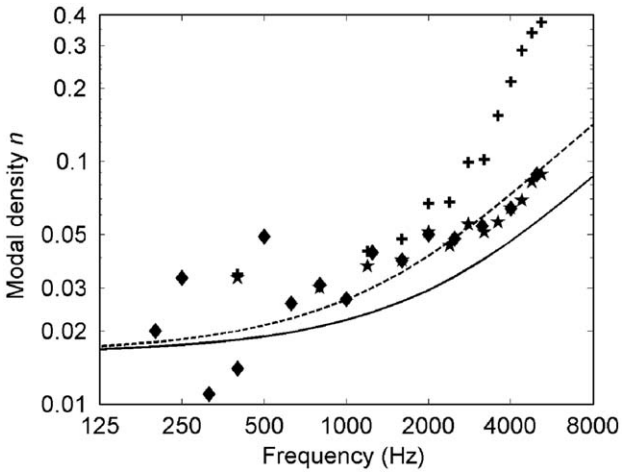

Fig. 4. Band-averaged modal density estimates for sandwich panel *C*: ♦ one-third octave bandwidth; ★ 400 Hz bandwidth; + 400 Hz bandwidth without mass correction; —— theoretical estimates by using Eq. (6) and $G_c = G_x$; – – – theoretical estimates by using Eq. (6) and $G_c = G_y$.

Markus, occur near to 1600 and 1000 Hz, respectively. In the low frequency region, the transverse motion of sandwich panels is determined by pure bending. Since the core thickness of panel *B* is one half of that of panel *C* and the properties of the face sheets of the two panels are similar, then the modal density of panel *B* is higher than that of panel *C* below 1000 Hz.

Theoretically higher out-of-phase shear modulus G_c yields lower modal density of the sandwich panels. The length of the two panels along the *x*-axis direction, l_x, is about twice of the length along the *y*-axis direction, l_y; See Fig. 2 and Table 1. The increment of the primary structural wave number component along the *x*-axis direction, Δk_x, is much less than that along the *y*-axis direction, Δk_y. The orthotropic behavior of the face sheet will increase the modal density of the sandwich panel [17]. These explain that why the experimental modal density values of panels *B* and *C* are near and a little higher than the theoretical predictions for $G_c = G_x$.

It was found that the effect of the contribution of the bending rigidity of the face sheets D_t on the modal density of sandwich panels *B* and *C* is negligible up to 6300 Hz. Eq. (6) provides accurate estimates for the two foam-filled honeycomb sandwich panels in the frequency range of interest. The difference between the prediction of modal density from Eq. (6) and that from Eqs. (4) and (5) is less than 0.002 up to 6300 Hz. Since the modal densities of the two panels are quite similar, and panel *B* is lighter than panel *C*, then the real component of the point mobility of panel *B* is larger than that of panel *C*.

4. Experimental total loss factors

Unlike modal densities, theoretical expressions for internal loss factors are not available. The loss factor of a structure can be obtained from the measurement of the force supplied to the structure and the spatially averaged square of the

normal velocity produced. In steady-state conditions, the average power input is equal to the average power dissipated, and thus the band-averaged loss factor is

$$\eta = \frac{1}{\Delta f}\int \frac{\overline{F^2(t)}\mathrm{Re}(Y)}{M_p\langle V^2(t)\rangle 2\pi f}\ \mathrm{d}f, \tag{17}$$

where F and Y are the actual or corrected force and point mobility of the structure.

As discussed in the previous section, the force measurement can be mass corrected. Then

$$\overline{F_c^2} = \frac{\overline{F_m^2}}{[1-\omega M\mathrm{Im}(Y_c)]^2 + [\omega M\mathrm{Re}(Y_c)]^2}. \tag{18}$$

where $\mathrm{Re}(Y_c)$ and $\mathrm{Im}(Y_c)$ can be determined from Eqs. (15) and (16).

In the case of the measurement of high frequency vibration of lightweight structures, considerable care should be taken when using an accelerometer because of the mass loading effect. Well below its resonance frequency, the accelerometer can be assumed to act as a pure mass. The velocity of the structure V_c can be assumed to be reduced to V_a by the presence of the accelerometer [31],

$$\frac{V_a}{V_c} = \frac{Z}{Z+\mathrm{i}\omega m_a}, \tag{19}$$

where Z is the mechanical impedance of the test element, and m_a is the accelerometer mass.

In this study, the mass loading of the accelerometer was assumed to be

$$\frac{V_a^2}{V_c^2} = \frac{1}{1+[\omega m_a\overline{\mathrm{Re}(Y_c)}]^2}, \tag{20}$$

where $\overline{Y_c}$ is the corrected point mobility of the panel and m_a the static mass of the accelerometer.

The corrected point mobilities of the sandwich panels were determined by following the procedure that is described in Section 3. An Endevco model 2226c piezoelectric accelerometer was attached to the panel with wax. The velocities of the sandwich panels were determined by measuring the panel responses with the accelerometer at five randomly chosen positions. The frequency spectral analysis resolution was chosen to be 1 Hz. The frequency analysis bandwidth of the loss factor analysis chosen was one-third octave. The loss factor estimates for panels B and C are shown in Fig. 5.

Since the real component of the point mobility of panel B is larger than that of panel C, then it was expected that accelerometer mass loading effects would corrupt the velocity measurements more with panel B than with panel C. It is seen that the mass loading effect of the accelerometer on the loss factor of panel C is negligible. It becomes apparent, however, at frequencies above 3150 Hz for panel B. The corrected loss factors of panels B and C are less than 0.03.

5. Experimental radiation loss factors

The radiation resistance of a structure, R_{rad}, in a reverberant field can be obtained experimentally as follows [21]:

$$R_{\mathrm{rad}} = \eta_{\mathrm{room}}\omega\frac{\langle P^2\rangle}{\rho c^2\langle V^2\rangle}V_{\mathrm{room}} = \frac{13.8S_p}{T_{\mathrm{room}}S_v\rho c^2}V_{\mathrm{room}}, \tag{21}$$

where S_p is the sound pressure spectral density function in the reverberation room and S_v the velocity spectral density function of the structure; T_{room} and V_{room} are the reverberation time and the volume of the room, respectively; and ρ and c are the mass density of air and the sound speed in air.

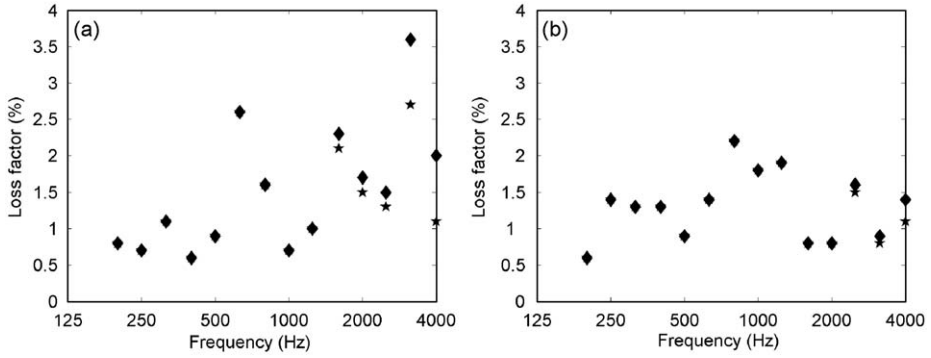

Fig. 5. Band-averaged total loss factor estimates for sandwich panels: (a) panel B and (b) panel C: ♦ without mass correction of the accelerometer; ★ with mass correction of the accelerometer.

The radiation resistance of a structure mounted between two reverberation rooms and excited by a shaker can be estimated experimentally [23],

$$R_{\mathrm{rad}} = \frac{13.8}{S_v \rho c^2}\left(\frac{S_{p_1}}{T_1}V_1 + \frac{S_{p_3}}{T_3}V_3\right). \tag{22}$$

It is noted that in both radiation resistance determinations, Eqs. (21) and (22), the radiation resistance is also termed as $R_{\mathrm{rad}}^{4\pi}$, because the effective radiating area of the panel is twice that of the area of the panel.

The radiation resistance of a baffled simply supported single-layer panel given by Maidanik [22] is, as corrected in Ref. [23],

$$R_{\mathrm{rad}}^{2\pi} = A_p \rho c \begin{cases} \sigma_{\mathrm{corner}} + \sigma_{\mathrm{edge}}, & f < f_c \\ \sqrt{l_x/\lambda_c} + \sqrt{l_y/\lambda_c}, & f = f_c \ \text{ with} \\ [1-(f_c/f)]^{-1/2}, & f > f_c \end{cases}$$

$$\sigma_{\mathrm{corner}} = \begin{cases} (\lambda_c \lambda_a / A_p)\alpha^2 (8/\pi^4)[(1-2\alpha^2)/\alpha/\sqrt{1-\alpha^2}], & f < f_c/2 \\ 0, & f > f_c/2 \end{cases},$$

$$\sigma_{\mathrm{edge}} = \frac{1}{4\pi^2}\frac{P\lambda_c}{A_p}\frac{(1-\alpha^2)\ln[(1+\alpha)/(1-\alpha)] + 2\alpha}{(1-\alpha^2)^{3/2}},$$

$$\lambda_a = \frac{c}{f}, \quad \lambda_c = \frac{c}{f_c}, \quad \alpha = \sqrt{\frac{f}{f_c}}, \tag{23}$$

where f_c and P are the critical frequency and the total length of the edges of the panel.

Gomperts [24] showed that the radiation efficiency of a baffled free-edge panel at frequencies well below the critical frequency is

$$\sigma_{\mathrm{baf,\ free}} = (2/5)(f/f_c)^2 \sigma_{\mathrm{baf,ss}} = (2/5)(f/f_c)^2(\sigma_{\mathrm{corner}} + \sigma_{\mathrm{edge}}),\ f \ll f_c. \tag{24}$$

When the panel is unbaffled, fluid flow around the panel edges reduces the sound radiation. Oppenheimer and Dubowsky [25] have provided an expression for the radiation efficiency for unbaffled simply supported panels,

$$\sigma_{\mathrm{unbaf,ss}} = F_{\mathrm{plate}}(F_{\mathrm{corner}}\sigma_{\mathrm{corner}} + F_{\mathrm{edge}}\sigma_{\mathrm{edge}}),\ f < f_c, \tag{25}$$

$$\text{with } F_{\mathrm{corner}} = \frac{13\alpha}{2(1+13\alpha)}, \quad F_{\mathrm{edge}} = \frac{49\alpha}{2(1+49\alpha)}, \quad F_{\mathrm{plate}} = \frac{k^4 A_p^2/(48\pi^2)}{1+k^4 A_p^2/(48\pi^2)},$$

where k is the wavenumber of sound in air.

The two foam-filled honeycomb sandwich panels were clamped sequentially between two reverberation rooms and excited by a B&K vibration exciter type 4809 to obtain their radiation resistances. The clamping reduced the dimensions of the panels to 0.88 m × 0.42 m. The sound pressure spectral density function in each room was determined by measuring the room responses with a microphone at eight positions. The velocity spectral density function of the panel was determined by measuring the panel responses with an accelerometer at eight positions. The mass loading effect of the accelerometer was included in the radiation resistance calculation. The frequency spectral analysis resolution was chosen to be 1 Hz. The frequency analysis bandwidth chosen was one-third octave. The measured radiation resistances of the two clamped sandwich panels are shown in Fig. 6.

As shown in Section 3, Eq. (6) offers accurate modal density estimates for the foam-filled honeycomb sandwich panels, then it was expected that Eq. (23) provides a good estimation of the radiation resistance of the thin sandwich panel *B*. The measured radiation resistance of the thick sandwich panel *C*, has a maximum value above the predicted critical frequency and this value is much smaller than the predicted value at the predicted critical frequency. This may be explained by the fact that there are not enough resonant modes near the critical frequency because of the relative small dimensions of the clamped panel *C*.

The radiation resistances of panels *B* and *C* with unbaffled free edges were also investigated. The panels were hung in a reverberation room and excited by a B&K vibration exciter type 4809. The sound pressure and velocity spectral density functions were obtained by following the same procedure for the baffled clamped model described early in this section. The mass loading effect of the accelerometer was included in the radiation resistance calculation.

Fig. 7 shows the experimental radiation resistances of the two foam-filled honeycomb sandwich panels with unbaffled free edges. The radiation resistances of the baffled free-edge panels and the unbaffled simply supported panels were calculated by using Eqs. (24) and (25).

It is seen that the measured radiation resistances of unbaffled free-edge sandwich panels are less than the predicted values of unbaffled simply supported single-layer panels, and slightly higher than those values for baffled free-edge single-layer panels. The maximum value of the measured radiation resistance of the unbaffled free-edge sandwich panels was found to occur at a frequency higher than that of the baffled clamped sandwich panels.

The radiation loss factor is determined from the radiation resistance by

$$\eta_{\mathrm{rad}} = \frac{R_{\mathrm{rad}}^{2\pi}}{\omega M_p}. \tag{26}$$

The radiation loss factor estimates for the sandwich panels *B* and *C* with baffled clamped edges and unbaffled free edges are shown in Fig. 8. The radiation loss factors of two sandwich panels, *B* and *C*, with clamped edges are much higher than those of the panels with free edges. The radiation loss factor for baffled clamped panel *B* is very high near its critical frequency. It is more than 0.02 in this region. The baffled clamped panel *C* has similar radiation loss factor values in the frequency band 315−2000 Hz.

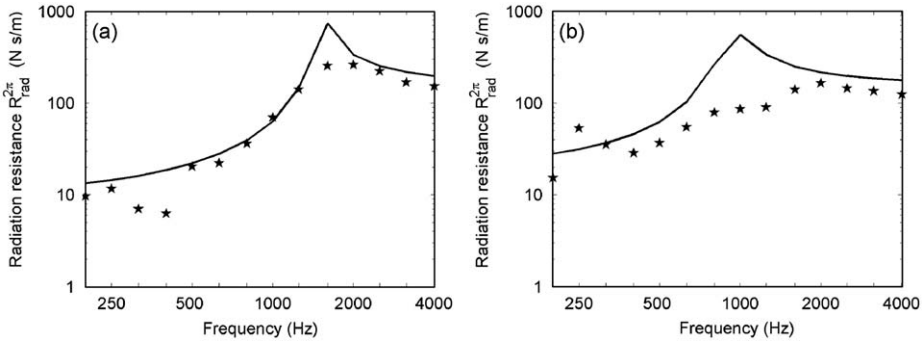

Fig. 6. Band-averaged radiation resistances for baffled clamped sandwich panels: (a) panel *B* and (b) panel *C*: ★ measured values with mass correction; —— one-third octave band-averaged theoretical estimates from Eq. (23).

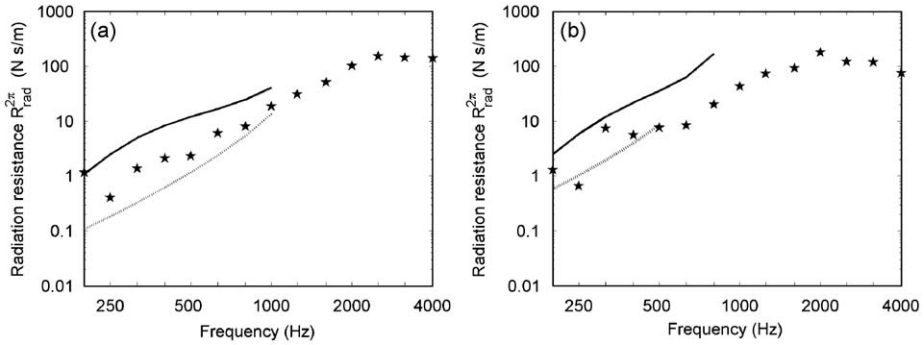

Fig. 7. Band-averaged radiation resistances for unbaffled free-edge sandwich panels: (a) panel *B* and (b) panel *C*: ★ measured values with mass correction; —— one-third octave band-averaged estimates for unbaffled simply supported panels from Eq. (25); ····· one-third octave band-averaged estimates for baffled free-edge panels from Eq. (24).

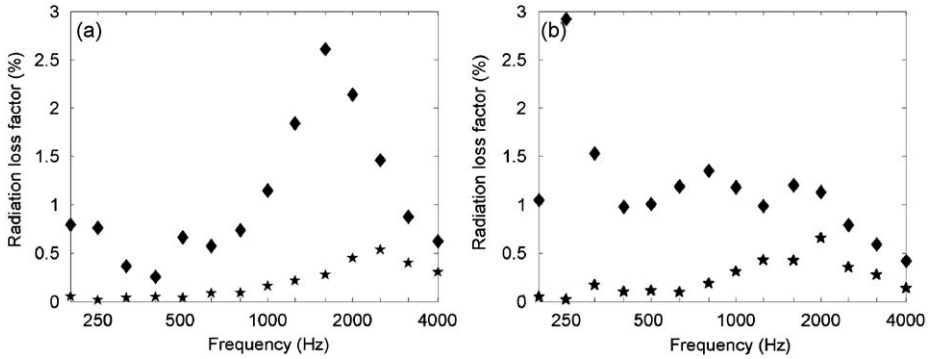

Fig. 8. Band-averaged radiation loss factor estimates for sandwich panels: (a) panel *B* and (b) panel *C*: ♦ with baffled clamped edges; ★ with unbaffled free edges.

6. Experimental internal loss factors

In the presence of a fluid medium, such as air, the experimental loss factor of a structure obtained from energy methods, is the sum of three forms of damping [32],

$$\eta = \eta_{\text{int}} + \eta_{\text{rad}} + \eta_j, \tag{27}$$

where η_{int} is the internal loss factor; η_{rad} the radiation loss factor; and η_j the loss factor associated with energy dissipation at the boundaries of the structural element.

The internal loss factor estimates for the two panels, *B* and *C*, were obtained by neglecting η_j, and are shown in Fig. 9. Since the total loss factor is for the unbaffled free-edge panel, η_{rad} is used for the radiation loss factor of the unbaffled free-edge panel in the computation of the internal loss factor. The internal loss factors of panels *B* and *C* are similar, and are less than 0.03 for the frequency band 200−4000 Hz.

7. Sound transmission loss of sandwich panels

The sound transmission loss measurements made on two sandwich panels were carried out in the Sound and Vibration Laboratory at Auburn University. The transmission suite consists of two adjacent 51.2 m^3 reverberation rooms. Each room has two walls made of wood with fiberglass filled in between them. The rooms are separated from each other by fiberglass, and are mounted on air bags. The panels were clamped in a frame between the two rooms. The panel edge conditions were intended to be fully fixed. The frame reduced the test dimensions of the panels to 0.84 m × 0.42 m. The sound transmission loss was measured according to the standard test method, ASTM E90-99. One-third octave bands of white noise were made in the source room with two loudspeakers and the sound pressure levels were measured at eight positions in each room. The mean square sound pressures in each room were averaged to provide the space-averaged values required.

The sound transmission loss for the two-room method is

$$\text{TL} = 10\log_{10}\frac{\langle p_1^2\rangle}{\langle p_3^2\rangle}\frac{A_p}{\tau A_p + S_3\alpha_3} = 10\log_{10}\left[\left(\frac{\langle p_1^2\rangle}{\langle p_3^2\rangle} - 1\right)\frac{A_p}{S_3\alpha_3}\right], \tag{28}$$

where $\langle p_1^2\rangle$ and $\langle p_3^2\rangle$ are the space-averaged mean square sound pressures in the source room and receiving room, respectively; S_3 the total surface area of the receiving room and α_3 the average absorption coefficient in the receiving room; and τ the sound transmission loss coefficient.

Eq. (28) can be written as

$$\text{TL} = L_1 - L_3 + 10\log_{10}\frac{A_p T}{0.161V_3} \quad \text{with } T = \frac{0.161V_3}{\tau A_p + S_3\alpha_3}, \tag{29}$$

where L_1 and L_3 are the space-averaged sound pressure levels measured in the two rooms; and *T* the reverberation time of the receiving room when a panel is clamped between the two rooms.

The power flow balance equations for the room-panel-room transmission suite, as illustrated in Fig. 10, can be written in matrix form [23],

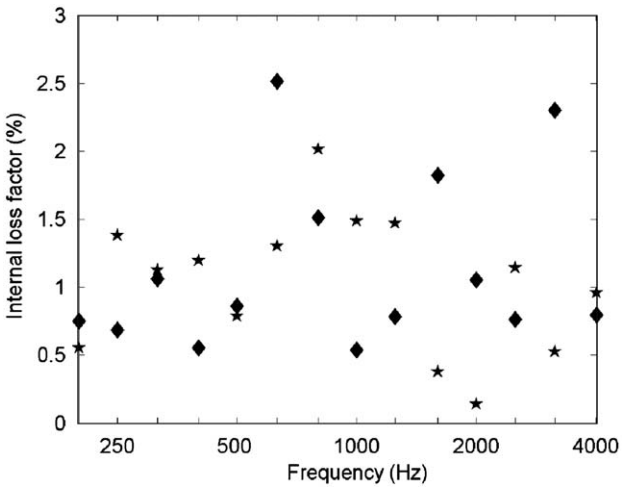

Fig. 9. Internal loss factor estimates for panels *B* and *C*: ♦ panel *B*; ★ panel *C*.

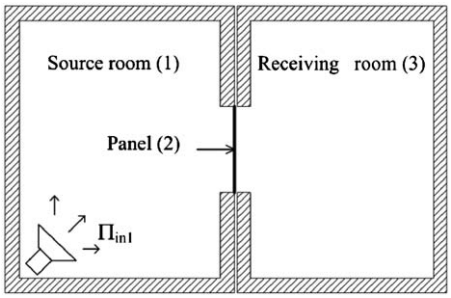

Fig. 10. The transmission suite.

$$\omega \mathbf{A} \begin{Bmatrix} E_1/n_1 \\ E_2/n_2 \\ E_3/n_3 \end{Bmatrix} = \begin{Bmatrix} \Pi_{in1} \\ 0 \\ 0 \end{Bmatrix}, \tag{30}$$

$$\text{with } \mathbf{A} = \begin{bmatrix} (\eta_1+\eta_{12}+\eta_{13})n_1 & -\eta_{12}n_1 & -\eta_{13}n_1 \\ -\eta_{21}n_2 & (\eta_2+\eta_{21}+\eta_{23})n_2 & -\eta_{23}n_2 \\ -\eta_{13}n_1 & -\eta_{23}n_2 & \eta_3 n_3+\eta_{13}n_1+\eta_{23}n_2 \end{bmatrix}.$$

Then the modal energy ratio is

$$\frac{E_1/n_1}{E_3/n_3} = 1 + \frac{2\eta_{rad}n_2\eta_3 n_3 + (\eta_3 n_3 + \eta_{rad}n_2)\eta_2 n_2}{\eta_{rad}^2 n_2^2 + \eta_{13}(2\eta_{rad}+\eta_2)n_1 n_2}, \tag{31}$$

with $\eta_{21} = \eta_{23} = \eta_{rad}$.

Since the mean square sound pressure ratio is equivalent to the sound energy density ratio between the two reverberation rooms, then the sound transmission loss for the SEA model of a transmission suite is

$$\text{TL} = 10\log_{10}\left[\frac{A_p T_3}{0.161V_3}\left(\frac{E_1/V_1}{E_3/V_3} - 1\right)\right], \quad \text{with } T_3 = \frac{0.161V_3}{S_3\alpha_3}, \tag{32}$$

where T_3 is the reverberation time of the receiving room.

The parameters used in the SEA calculation were evaluated both experimentally and theoretically in the calculations of the sound transmission loss for the two sandwich panels. The internal loss factor of the receiving room, η_3, was determined from the reverberation time of the receiving room:

$$\eta_3 = \frac{2.2}{fT_3}. \tag{33}$$

The reverberation time of the receiving room was obtained by averaging the reverberation times at eight randomly chosen positions. The modal densities of the two reverberation rooms, n_1 and n_3, were obtained from the following equation:

$$n(f) = \frac{4\pi f^2 V}{c^3} + \frac{\pi f S}{2c^2} + \frac{P}{8c}, \tag{34}$$

where V is the volume of the room; S the total surface area; and P the total length of the edges. The values of the radiation loss factor, η_{rad}, used were determined from Eq. (23). The values of the coupling loss factor, η_{13}, were determined from the field incidence mass law transmission coefficient. Based on the experimental modal density estimates, Fig. 3, the values of modal density, n_2, of panel B used were the modal density for simply supported conditions and were derived from Eqs. (4) and (5) with $G_c = G_x$. Similarly, based on Fig. 4, the values of modal density, n_2, of panel C used were the modal density for simply supported conditions and were derived from Eqs. (4) and (5) with $G_c = G_y$. The sound transmission loss estimates of the panels were generated for two different values of internal loss factor of the panels, $\eta_2 = 0.01, 0.03$. The sound transmission loss values of panels B and C are shown in Figs. 11 and 12.

The first resonance frequencies of panels B and C are in the one-third octave bands with center frequencies of 250 and 315 Hz, respectively. The experimental transmission loss curve for panel B is near the field incidence mass law curve at frequencies well below the critical frequency, while that of panel C is significantly lower than the field incidence mass law curve and is strongly influenced by its resonant modes. Below their first resonance frequencies, the two panels are in their stiffness controlled regions. The coincidence dips of the two panels are not as apparent as those of metal panels and they do not return rapidly towards the mass law curves as the frequency increases above the critical frequency. The experimental transmission loss values are about 15 dB lower from the field incidence mass law curves. The SEA estimates for both panels are in good agreement with the experimental results well above the critical frequency. SEA also provides reasonable predictions for the sound transmission loss of panel B below its critical frequency. The discrepancy above the first resonance frequency and below the critical frequency for panel C is thought to be caused by insufficient panel modes in

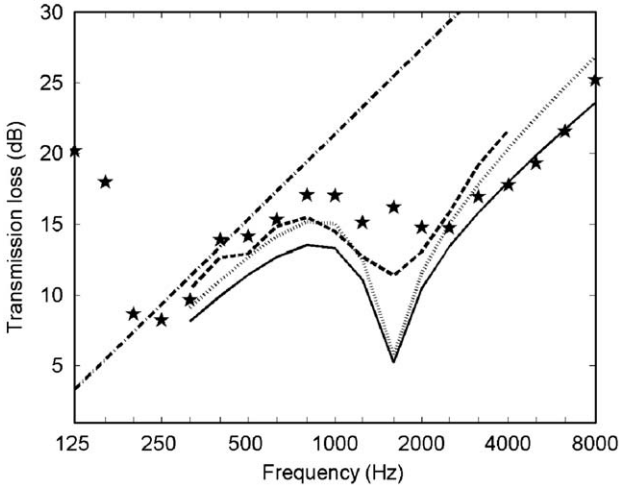

Fig. 11. Sound transmission loss values of panel *B*: ★ measured values; —— $\eta_2 = 0.01$; ····· $\eta_2 = 0.03$; – – – $\eta_2 = 0.03$ with the measured values of η_{rad}; – · – · – field incidence mass law.

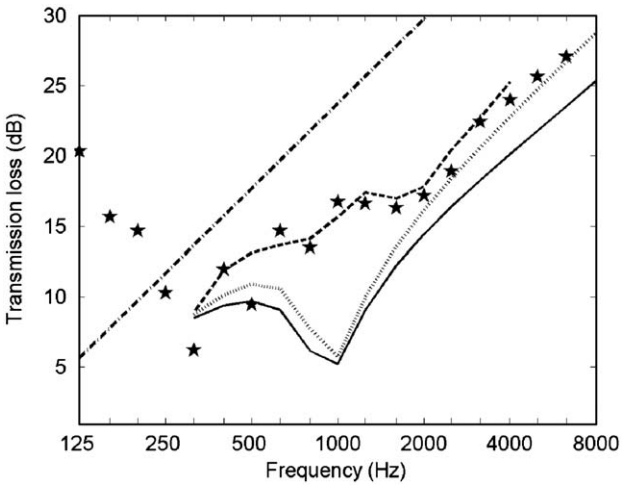

Fig. 12. Sound transmission loss values of panel *C*: ★ measured values; —— $\eta_2 = 0.01$; ····· $\eta_2 = 0.03$; – – – $\eta_2 = 0.03$ with the measured values of η_{rad}; – · – · – field incidence mass law.

one-third octave bands. It is seen that the SEA sound transmission loss estimates are more sensitive to the radiation loss factor than the internal loss factor of the panels near to the critical frequency. The disagreements near to the critical frequency are reduced when the measured values of the radiation loss factor η_{rad} near to the critical frequency are used in the calculation.

8. Conclusions

Comparisons between the experimental and predicted sound transmission loss values obtained from statistical energy analysis have been made and presented for two foam-filled honeycomb sandwich panels. The predicted and experimental transmission loss values of the sandwich panels are in better agreement when the measured radiation loss factor values are used near to the critical frequency instead of the theoretical values for single-layer panels.

A closed-form expression for the modal densities of sandwich panels developed from a typical sixth-order governing equation for sandwich panels with stiff cores has been presented. It was found that in high frequency range, the modal density derived from this closed-form expression can be as little as one half of the approximate modal density that is obtained from a fourth-order governing equation for a traditional honeycomb sandwich panel.

The radiation loss factors of clamped sandwich panels are large near to the critical frequency, especially for thin sandwich panels; while the radiation loss factors of unbaffled free-edge sandwich panels are much smaller than those of baffled clamped sandwich panels. The internal loss factors are dominant in the total loss factor estimates for the unbaffled

free-edge sandwich panels studied. The expression for the radiation resistance of sandwich panels is a subject that requires further study.

References

[1] M.J. Crocker (Ed.), *Handbook of Noise and Vibration Control*, Wiley, New Jersey, 2007.
[2] M.D. Rao, Recent applications of viscoelastic damping for noise control in automobiles and commercial airplanes, *Journal of Sound and Vibration* 262 (2003) 457–474.
[3] R.B. Randall, The application of fault simulation to machine diagnostics and prognostics, *International Journal of Acoustics and Vibration* 14 (2009) 81–89.
[4] N.B. Roozen, J. van der Oetelaar, A. Geerlings, T. Vliegenthart, Source identification and noise reduction of a reciprocating compressor: a case history, *International Journal of Acoustics and Vibration* 14 (2009) 90–98.
[5] J. Tuma, Gearbox noise and vibration prediction and control, *International Journal of Acoustics and Vibration* 14 (2009) 99–108.
[6] Z. Li, M.J. Crocker, A review of vibration damping in sandwich composite structures, *International Journal of Acoustics and Vibration* 10 (2005) 159–169.
[7] K.H. Hornig, G.T. Flowers, Performance of heuristic optimisation methods in the characterisation of the dynamic properties of sandwich composite materials, *International Journal of Acoustics and Vibration* 12 (2007) 60–68.
[8] Z. Li, M.J. Crocker, Effects of thickness and delamination on the damping in honeycomb-foam sandwich beams, *Journal of Sound and Vibration* 294 (2006) 473–485.
[9] T. Chavan, D.N. Manik, Optimum design of vibro-acoustic systems using SEA, *International Journal of Acoustics and Vibration* 13 (2008) 67–81.
[10] L. Cremer, M. Heckl, E.E. Ungar, *Structure-Borne Sound*, Springer, New York, 1973.
[11] B.L. Clarkson, R.J. Pope, Experimental determination of modal densities and loss factors of flat plates and cylinders, *Journal of Sound and Vibration* 77 (1981) 535–549.
[12] K.T. Brown, Measurement of modal density: an improved technique for use on lightly damped structures, *Journal of Sound and Vibration* 96 (1984) 127–132.
[13] K.T. Brown, M.P. Norton, Some comments on the experimental determination of modal densities and loss factors for statistical energy analysis application, *Journal of Sound and Vibration* 102 (1985) 588–594.
[14] P.R. Keswick, M.P. Norton, A comparison of modal density measurement techniques, *Applied Acoustics* 20 (1987) 137–153.
[15] B.L. Clarkson, M.F. Ranky, Modal density of honeycomb plates, *Journal of Sound and Vibration* 91 (1983) 103–118.
[16] D.J. Mead, S. Markus, The force vibration of a three-layer, damped sandwich beam with arbitrary boundary conditions, *Journal of Sound and Vibration* 10 (1969) 163–175.
[17] K. Renji, P.S. Nair, Modal density of composite honeycomb sandwich panels, *Journal of Sound and Vibration* 195 (1996) 687–699.
[18] N.S. Ferguson, B.L. Clarkson, The modal density of honeycomb shells, *Journal of vibration, Acoustics, Stress, and Reliability in Design* 108 (1986) 399–404.
[19] M.F. Ranky, B.L. Clarkson, Frequency average loss factors of plates and shells, *Journal of Sound and Vibration* 89 (1983) 309–323.
[20] K. Renji, S.S. Narayan, Loss factors of composite honeycomb sandwich panels, *Journal of Sound and Vibration* 250 (2002) 745–761.
[21] R.H. Lyon, G. Maidanik, Power flow between linearly coupled oscillators, *Journal of the Acoustical Society of America* 34 (1962) 623–639.
[22] G. Maidanik, Response of ribbed panels to reverberant acoustic fields, *Journal of the Acoustical Society of America* 34 (1962) 809–826.
[23] M.J. Crocker, A.J. Price, Sound transmission using statistical energy analysis, *Journal of Sound and Vibration* 9 (1969) 469–486.
[24] M.C. Gomperts, Radiation from rigid baffled, rectangular plates with general boundary conditions, *Acustica* 30 (1974) 320–327.
[25] C.H. Oppenheimer, S. Dubowsky, A radiation efficiency for unbaffled plates with experimental validation, *Journal of Sound and Vibration* 199 (1997) 473–489.
[26] E.C. Sewell, Transmission of reverberant sound through a single-leaf partition surrounded by an infinite rigid baffle, *Journal of Sound and Vibration* 12 (1970) 21–32.
[27] C.L. Dym, M.A. Lang, Transmission of sound through sandwich panels, *Journal of the Acoustical Society of America* 56 (1974) 1523–1532.
[28] C.L. Dym, D.C. Lang, Transmission loss of damped asymmetric sandwich panels with orthotropic cores, *Journal of Sound and Vibration* 88 (1983) 299–319.
[29] J.A. Moore, R.H. Lyon, Sound transmission loss characteristics of sandwich panel constructions, *Journal of the Acoustical Society of America* 89 (1991) 777–791.
[30] E. Nilsson, A.C. Nilsson, Prediction and measurement of some dynamic properties of sandwich structures with honeycomb and foam cores, *Journal of Sound and Vibration* 251 (2002) 409–430.
[31] E.A. Starr, *Noise and Vibration Control*, McGraw-Hill, New York, 1971.
[32] M.P. Norton, *Fundamentals of Noise and Vibration Analysis for Engineers*, Cambridge University Press, Cambridge, New York, 1989.